



Alternating defects and egg and dart textures in de-wetted stripes of discotic liquid crystal

Jonathan P. Bramble, Daniel J. Tate, Stephen D. Evans, John E. Lydon & Richard J. Bushby

To cite this article: Jonathan P. Bramble, Daniel J. Tate, Stephen D. Evans, John E. Lydon & Richard J. Bushby (2022) Alternating defects and egg and dart textures in de-wetted stripes of discotic liquid crystal, *Liquid Crystals*, 49:4, 543-558, DOI: [10.1080/02678292.2021.1983048](https://doi.org/10.1080/02678292.2021.1983048)

To link to this article: <https://doi.org/10.1080/02678292.2021.1983048>



© 2021 The Author(s). Published by Informa UK Limited, trading as Taylor & Francis Group.



Published online: 14 Oct 2021.



Submit your article to this journal [↗](#)



Article views: 407



View related articles [↗](#)



View Crossmark data [↗](#)

Alternating defects and egg and dart textures in de-wetted stripes of discotic liquid crystal

Jonathan P. Bramble^a, Daniel J. Tate^b, Stephen D. Evans^a, John E. Lydon^c and Richard J. Bushby^b

^aSchool of Physics and Astronomy, University of Leeds, Leeds, UK; ^bSchool of Chemistry, University of Leeds, Leeds, UK; ^cFaculty of Biological Sciences, University of Leeds, Leeds, UK

ABSTRACT

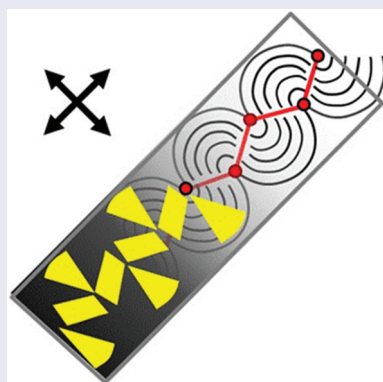
Isotropic phase de-wetting of discotic liquid crystals on a surface patterned with alternating $\sim 5\text{--}10\ \mu\text{m}$ wide wetting and de-wetting stripes results in the formation of long narrow droplets. On slow cooling into the columnar phase, the liquid crystal aligns such that the columns lie either across or along the stripes. However, if the stripes are wider and/or the cooling rate is too fast, defects appear. When there are many such defects, the result is complex zigzag and wavy line optical textures, which are reminiscent of the egg and dart friezes associated with classical architecture. To a first approximation, all of these patterns can be seen as joined up fragments of developable domains in which the columns either circle a defect or propagate in a straight line. They are built up from motifs that involve bend but not splay or twist deformations; deformations that leave the two-dimensional lattice of the columnar phase unchanged. As is shown, these basic circular and straight-line motifs can be combined in a variety of different ways along the stripe but, in all of these, it is found that the defects alternate from side to side.

ARTICLE HISTORY

Received 24 August 2021
Accepted 16 September 2021

KEYWORDS


Discotic liquid crystals;
columnar phases; optical
textures; developable
domains; de-wetting



1. Introduction

Understanding how the director fields of liquid crystals (LCs) respond to confinement in thin films, fibres, droplets etc. is fundamental to our use of these materials in displays, in optical compensating films [1], in the production of high tensile strength fibres [2–4], and in chemical and biological sensors [5–7]. In the absence of stress or flow, the director fields observed depend not only on the nature and scale of the confinement but also on the nature of the LC itself; on its anchoring energies and elastic constants [8]. In the case of columnar phases of discotic LCs, much of this behaviour is dominated by strong planar anchoring at an air interface [9–12] and the fact that bend deformations are

energetically much less costly than splay or twist deformations of the director field. This, in turn, relates to the fact that (locally constant curvature) bend deformations do not change the two-dimensional lattice; they do not change the spacing between the columns, whereas this is not true for splay and twist deformations. Hence, the behaviour of columnar phases is dominated by the formation of ‘developable domains’ [13–15]. Within these the columns propagate either in a straight line or along a circular path, Figure 1. This contrasts to the situation for lamellar phases of smectic LCs where behaviour in the bulk is dominated by the formation of Dupin cyclide/focal conic structures. In the first case, the formation of developable domains is driven by the need to

CONTACT Richard J. Bushby  r.j.bushby@leeds.ac.uk

© 2021 The Author(s). Published by Informa UK Limited, trading as Taylor & Francis Group.
This is an Open Access article distributed under the terms of the Creative Commons Attribution License (<http://creativecommons.org/licenses/by/4.0/>), which permits unrestricted use, distribution, and reproduction in any medium, provided the original work is properly cited.

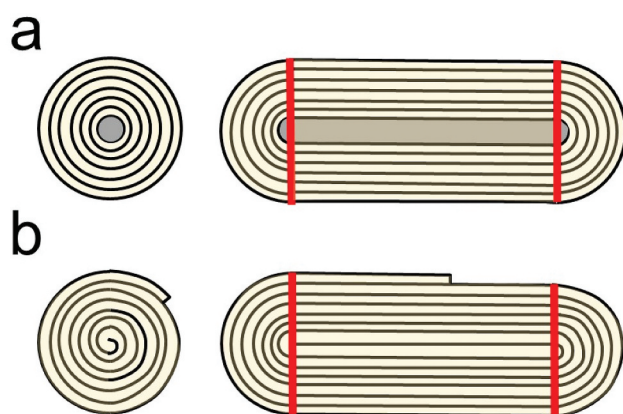


Figure 1. (Colour online) Schematic representations of developable domains viewed perpendicular to the $s = 1$ or $s = \frac{1}{2}$ defect lines (see text). The solid red lines represent a transition from circular to straight line propagation of the columns. (a) ‘Traditional’ representation in which the shaded areas represent areas of disorder or of escape into the third dimension (b) equivalent spiral structures with no disorder or escape in the centre.

maintain constant column–column separation whereas, in the second case, the formation of focal conic structures is driven by the need to maintain zero net surface curvature of equally spaced smectic layers. Developable domains are characterised by straight line $s = 1$ defects (or by a pair of straight line $s = \frac{1}{2}$ defects) and a perpendicular projection of the director field has traditionally been represented by drawing circular or semi-circular lines around these defects, Figure 1(a). Often the centre of the domain was shaded to indicate the belief that, in the centre, there was perhaps escape of the director field into the third dimension or that there was a region of high disorder [15]; it being assumed that, in the centre, the energy associated very high curvature would prove to be prohibitively high. However, in the case where these structures have been characterised by high-resolution AFM it was found that the columns were only approximately represented by a set of parallel rings. Actually, they spiralled very gently in towards the centre. It was also seen that they reached right into the centre; that there was no apparent disorder or escape of the director field in the centre of the domain (Figure 1 (b)) [16].

This paper is concerned with the way that developable domains appear and the way they interact with each other in thin ‘open to the air’ films and in long narrow de-wetted droplets. In the latter case the way in which the domains match up with each other results in a variety of zig-zag and wavy-line optical textures in which the defects are seen to alternate from one side of the droplet to the other. The discogens used in this study and specifically discussed in this paper are shown

in Figure 2. However, the columnar phases of a wide range of different discotic LCs behave in a very similar manner. The case of the open-to-the-air films is discussed first.

2. Materials and methods

2.1. Materials

The syntheses and the characterisation of the LCs used has been described previously [17–20].

2.2. Alignment of the LCs in thin open films and on patterned substrates

For the alignment in thin open films, glass slides were cleaned by sonication in Decon 90 and deionised water solution at 60°C for 1 h before rinsing with water, methanol, and IPA and drying in an oven at 100°C for 2 h. A small sample of the LC was added and the slide heated until the LC reached its isotropic phase, which was bladed to produce the film. It was then slowly cooled into the columnar phase.

On the patterned substrates, once the sample had been spread out, a spontaneous de-wetting was observed leading to an array of long narrow droplets

2.3. Microscopy observation

This was carried out using a polarised light microscope (POM) from either Leica Microsystems Ltd or from Nikon Instruments Inc., equipped with a pair of linear polarisers, a Nikon D3000 or Olympus SP350 camera and a Linkam T95 Peltier hot stage. As required, a first-order retardation plate (λ wave plate Olympus, Japan) was placed in the optical path of the microscope, with its slow axis at 45° to the polariser.

2.4. Fabrication of the patterned substrates

For the transmission mode images (Figures 6, 7, 9–11) the patterned substrates were made using the positive photoresist S1813 as described in Crystals [21]. The substrates were glass, the high-energy stripes were glass and the low-energy stripes were a silane-on-glass self-assembled monolayer, which was made from 1 H, 1 H, 2 H, 2 H-perfluorodecyltrichlorosilane.

For the reflection mode images (Figures 13–17), organosilane self-assembled monolayers created on the native SiO₂ surface of silicon wafers (Rockwood, USA) were patterned using deep UV photolithography as described in Advanced Functional Materials [22]. In

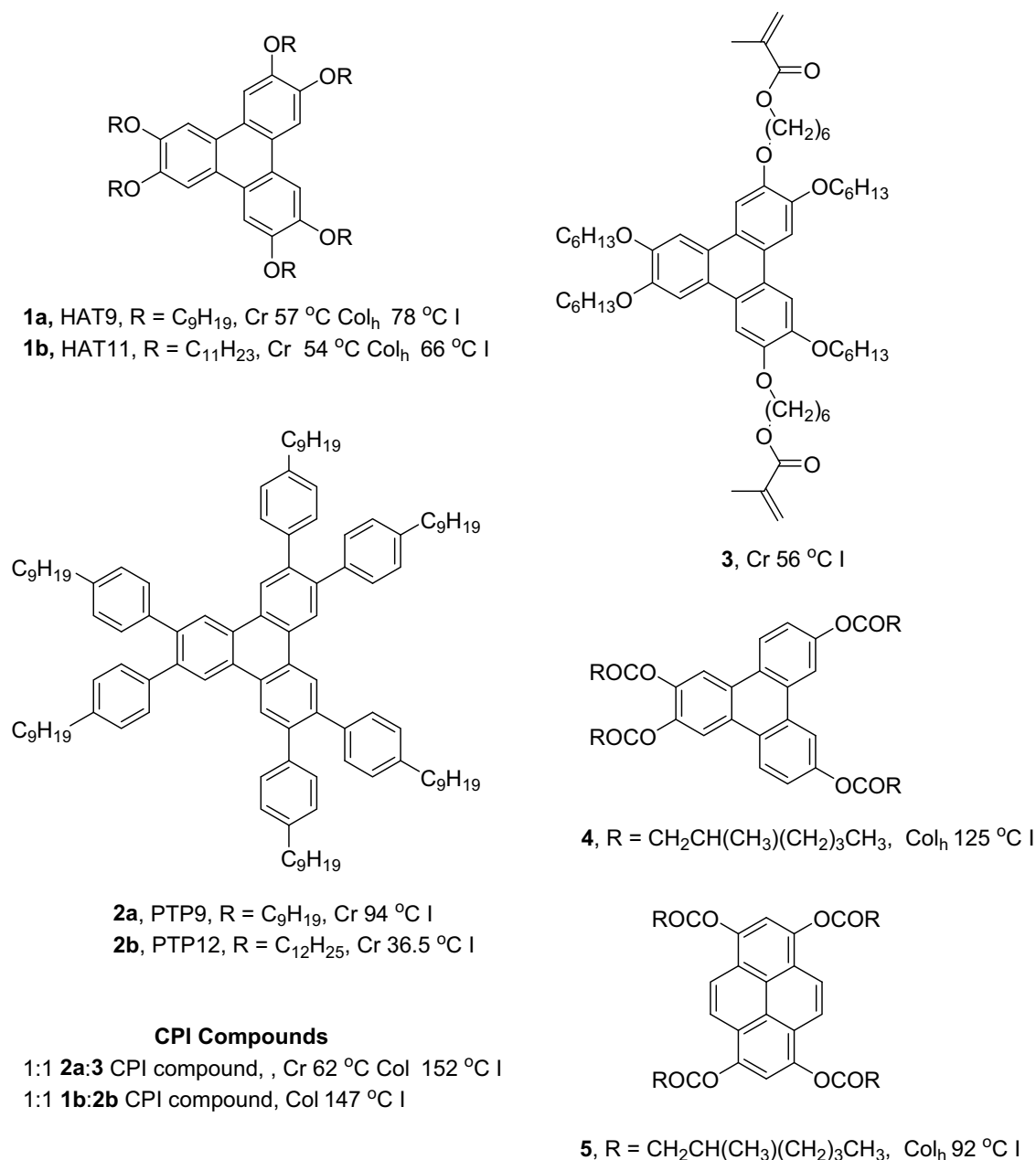


Figure 2. Molecular formulae and transition temperatures for the discogens and CPI compounds discussed in this paper.

this case, the high-energy stripes were SiO₂ and the low-energy stripes were created from perfluorodecyltrimethylchlorosilane (Fluorochem Ltd.).

3. Results and discussion

3.1. Optical textures observed for thin 'open-to-the-air' films

Whereas the discotic LC field has followed the precedent set by the much-longer established calamitic LC field and has concentrated on the optical textures

observed when samples are sandwiched between glass slides, in the case of discotic LCs, the textures observed for thin films, which are open-to-the-air can be much more informative [13]. However, to obtain useful textures requires a very clean high-energy surface (otherwise a thin film is unstable and it de-wets to form thick irregularly-shaped droplets) and often some experimentation is needed to obtain the correct thickness, cooling rate etc.

When sandwiched between glass slides, columnar phases often anchor in a perpendicular (homeotropic) manner so that (using crossed polarisers) the sample

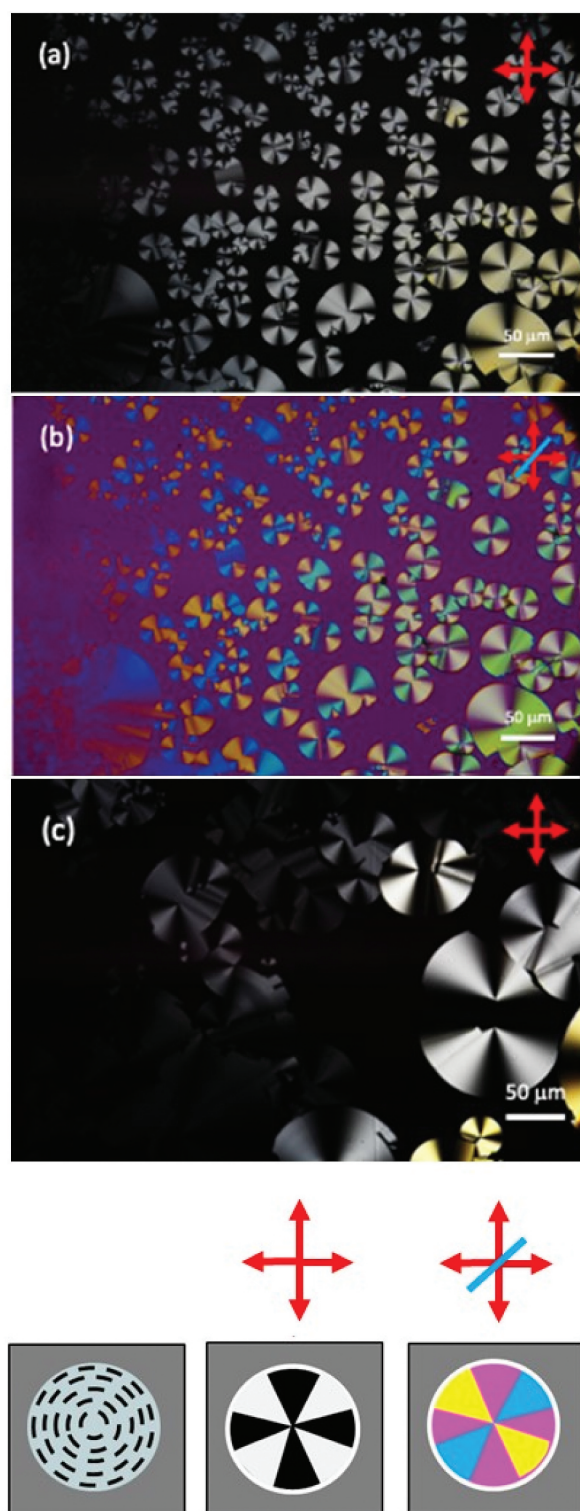


Figure 3. (Colour online) (Above) A thin open film of 1:1 HAT11:PTP12 at 95°C cooled from the isotropic to the columnar phase at 5°C/min and observed in transmission mode (x50 objective) (a) with crossed polarisers and (b) with crossed polarisers and an added wave-plate. The blue line indicates the orientation of the slow axis of the wave-plate. Note that, for this sample, the Col/I transition occurs at 147°C and the black/magenta 'background' is homeotropic columnar. (c) Same area of the same sample but at 110°C and with a cooling rate from the isotropic phase of 0.5°C/min. Crossed polarisers. (Below) Orientation diagram for interpreting the colours seen using crossed polarisers (centre) and a red 1λ plate (right, oriented as shown) for a developable domain viewed along the $s = 1$ defect line.

appears black. Alternatively, there is planar/tilted anchoring which leads to a disordered array of segments of developable domains giving a ‘mosaic’ or a ‘fan’ texture. Except in those rare cases where the $s = 1$ or $s = \frac{1}{2}$ disclination lines of these domains lie parallel to the glass, when highly characteristic straight-line multi-coloured ‘medal ribbon’ features can be seen [20], these textures are not clearly indicative of a columnar phase. The fan texture formed by a columnar phase looks very like the fan texture of a smectic A phase and, unfortunately, they are often even labelled as ‘focal conic’ or ‘pseudo-focal conic’. This is despite the fact that the underlying structures that give rise to them are developable domains and not focal conics!

Because, in thin open-to-the-air films, the alignment of the domains is dominated by the air interface (because the domains form with the columns parallel and the defects perpendicular to the surface) open-to-the-air films often give more distinctive textures. Commonly, fan-like textures are observed and this case has been discussed in detail by Bouligand [13]. Another texture, which is often observed is shown in Figure 3. In this particular case, the Col_h phase of the CPI compound [23,24] 1:1 HAT11:PTP12 was cooled from the isotropic phase at 5°C/min. Using crossed polarisers, what is seen in Figure 3(a) is bright, sharp-edged discs each displaying a Maltese Cross (or ‘stretched’ Maltese Cross) set in a black background. What is seen is developable domains with their $s = 1$ or $s = \frac{1}{2}$ axes perpendicular to the surface and the LC director/the columns parallel to the air interface. As expected, the domains with an $s = 1$ defect line are circular. When a red first-order λ wave plate is placed in the optical path of the microscope, with the slow axis of the retarder at +45°, as shown in Figure 3(b), the lower right and upper left quadrants of the domains translate from first order grey to first order yellow and the upper right and lower left quadrants from first order grey to second order blue confirming that, to a first approximation, the columns circle around the central defect(s); they do not radiate outwards [22]. The colour of the background translates from black to magenta. In general, for columnar phases, such a texture can indicate developable domains that are growing from an isotropic phase or domains trapped within a background homeotropic Col_h phase. Since CPI compounds are ‘compounds’ in the Phase Rule sense of that word and do not show a two-phase region at the Col_h/I transition [23] and since the images in Figure 5(a,b) were taken ~50°C below the transition temperature the second possibility applies in this case. The way in which this situation arises has been studied in detail by Grelet and Boch

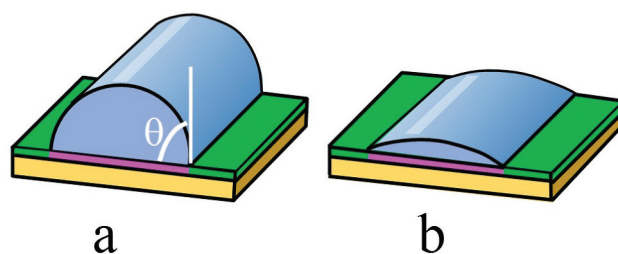


Figure 4. (Colour online) Schematic of droplets produced by dewetting of a liquid on a surface patterned with narrow hydrophilic/hydrophobic stripes. Mauve = hydrophilic/high energy surface. Green = hydrophobic/low energy surface. (a) $\theta = 90^\circ$ (hemicylinder) (b) $\theta < 90^\circ$ (shallow longitudinal section of a cylinder).

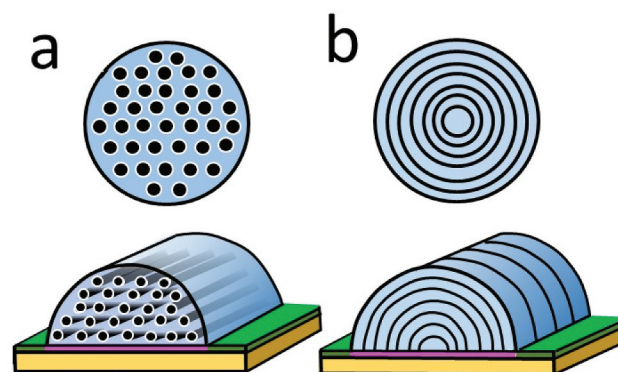


Figure 5. (Colour online) (Above) Director fields commonly seen for columnar phases of discotic LCs under cylindrical confinement (shown in cross-sections, **a** = uniform axial, **b** = planar radial). (Below) Equivalent director fields in the de-wetted stripes (shown in profile).

using the discogens 4 and 5 [25]. They showed that, when the film is very thin and the cooling rate is very slow, the whole sample aligns parallel to the surface but if the film is a little thicker or the cooling rate a little faster, restructuring at the air interface is incomplete and areas with alignment parallel to the surface become ‘trapped’ in a homeotropic matrix. In such cases, with the wave-plate in place, when a blade or needle is drawn through the homeotropic region, the columns align with the direction of shear giving a yellow or blue line (depending on whether the scratch is aligned or perpendicular to the slow axis of the compensator).

There are two, highly characteristic features to note in the textures shown in Figure 3. The first is the sharpness of the edges of the domains. This arises because the director fields either side of the interface are orthogonal to each other. This contrasts sharply with the way in which developable domains grow in the case of the de-wetted stripes, which are discussed in the next section, where they are not orthogonal and the boundaries of the domains are very diffuse. The second characteristic

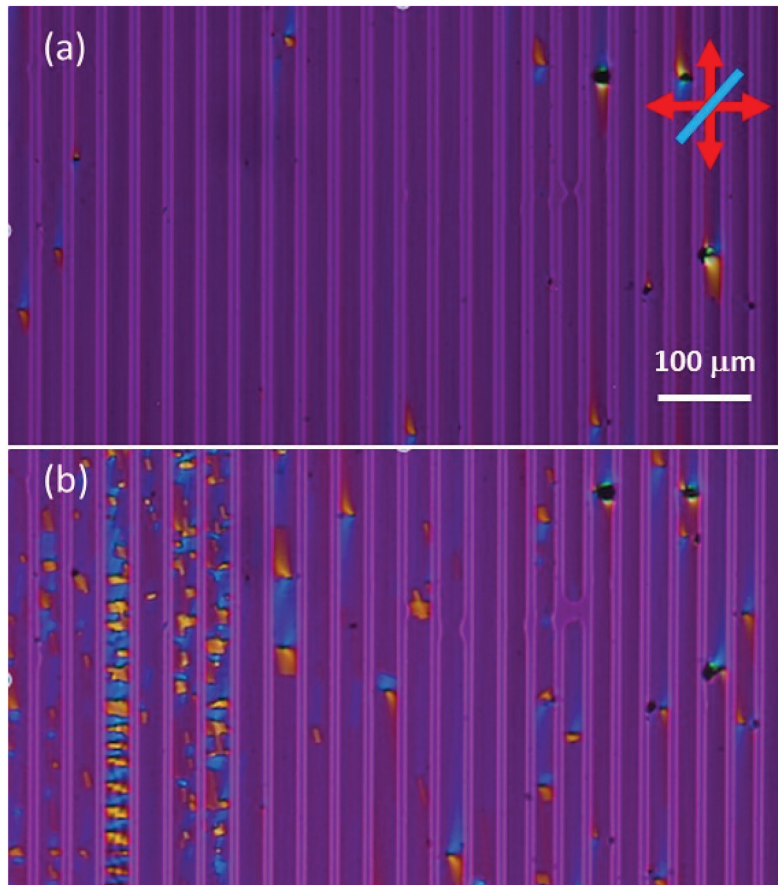


Figure 6. (Colour online) De-wetted sample of HAT11 on a patterned glass substrate which gives 25 μm (left side of the images) and 20 μm (right side of the images) wide droplets with 10 μm wide spaces between them. Both images are for the same area of the sample and were taken with the LC in its Col_h phase at 60°C. (a) Cooling rate from the isotropic phase of 0.1°C/min. (b) Cooling rate of 1°C/min (Same area of the sample). Transmission mode images, crossed polarisers with an added wave-plate. The blue line indicates the orientation of the slow axis of the wave-plate.

feature shown in Figure 3 is that, as well as some $s = 1$ defects (four brush defects) there are also many domains with pairs of $s = \frac{1}{2}$ defects (two brush defects). This contrasts to the texture observed for smectic A LCs when the focal conic structures are viewed ‘end-on’. In this case, the domains show just four brush defects [26,27].

A further aspect of the behaviour of these ‘flat’ open-to-the-air films that is relevant to understanding the behaviour in the de-wetted stripes is the effect of cooling rate on the number of defects. When the sample is cooled more slowly (0.1°C/min, Figure 3(c)), fewer developable domains are observed and these much larger. This is a situation analogous to that often seen when materials crystallise from solution or from the isotropic phase, where slower cooling often results in fewer, larger crystals. Because, when this sample was cooled at 0.1°C/min to 95°C the developable domains grew to fully cover the field of view, the image shown in Figure 3(c)

was taken at 110°C but otherwise this image is wholly comparable to those shown in Figure 3(a,b); it is the same area of the same sample.

3.2. Optical textures observed for de-wetted stripes

Production of the thin de-wetted stripes of DLCs, which is the main theme of this paper, relies on isotropic phase de-wetting of a thin film of the LC on a surface patterned with narrow alternating stripes of high energy (hydrophilic) and low energy (hydrophobic) surface [21,22]. On such a surface there is spontaneous de-wetting of the LC onto the high energy stripes. On these small scales, the profile of the droplets formed is determined by surface tension leading to even curvature at the air to LC interface; Figure 4 [21]. In the case of a previous study of columnar discotic LCs using stripes $\sim 10 \mu\text{m}$ wide we found droplet profiles that approached those of a hemi-cylinder

(Figure 4(a), contact angles approaching 90°) [22] but in more recent studies of calamitic nematic LCs on stripes $\sim 20\ \mu\text{m}$ wide we have found very low contact angles ($\sim 10^\circ$); much more shallow longitudinal sections of a cylinder. (Figure 4(b)) [21].

Because of the importance of understanding director fields in LC-derived high-tensile strength fibres like carbon fibre [2,3], Kevlar [4] and spider silk [28,29], cases where the director field of a LC is subject to cylindrical confinement have been investigated in detail both from a theoretical and from an experimental standpoint. In the case of columnar phases of discotic LCs the commonly observed director fields are ‘uniform axial’ (all of the columns parallel to the axis of the fibre/capillary) and ‘planar radial’ (a single developable domain with an $s = 1$ or pair of $s = 1/2$ defect lines running down the middle), Figure 5 [30–37]. In the case of a fibre, both of these director fields allow the preferred planar alignment of the LC at the air interface. The first director field involves no excess elastic energy and the latter only the low excess energy associated with uniform bend deformations. The director fields observed in the de-wetted stripes are probably simple variants on this theme. Hence, some columnar phases align in these stripes with the director parallel to the direction of the stripe (a section of the ‘uniform axial’

director field) but more commonly, when these stripes are observed using polarised optical microscopy, the director field (in projection) is perpendicular to the direction of the stripes. This is probably a longitudinal section of a developable domain. In a hemi-cylindrical stripe, this would allow the columnar phase to adopt its preferred perpendicular alignment on the solid surface (Figure 5(b)); at lower contact angles the alignment is tilted.

Such isotropic phase de-wetting is one of the most effective ways of producing samples in which all of the columns lie in the plane and they all ‘point’ in the same direction. However, the production of high-quality, uniform alignment depends on using very narrow stripes (usually $10\ \mu\text{m}$ or less wide) and on cooling slowly (usually $<1^\circ\text{C}/\text{min}$) [22]. Wider stripes and/or faster cooling leads to defects (compare Figure 6(a,b)). Since wider stripes tend to lead to flatter droplets and lower contact angles, the dependence of the number of defects on the width of the stripes is easy to understand. The azimuthal anchoring strength is determined by Berreman factors [38] which become weaker as the curvature of the surface decreases. However, if the cooling rate is slow enough, even on $25\ \mu\text{m}$ wide stripes, the alignment is good, and there are only a few defects, Figure 6(a). The increased number of defects seen on

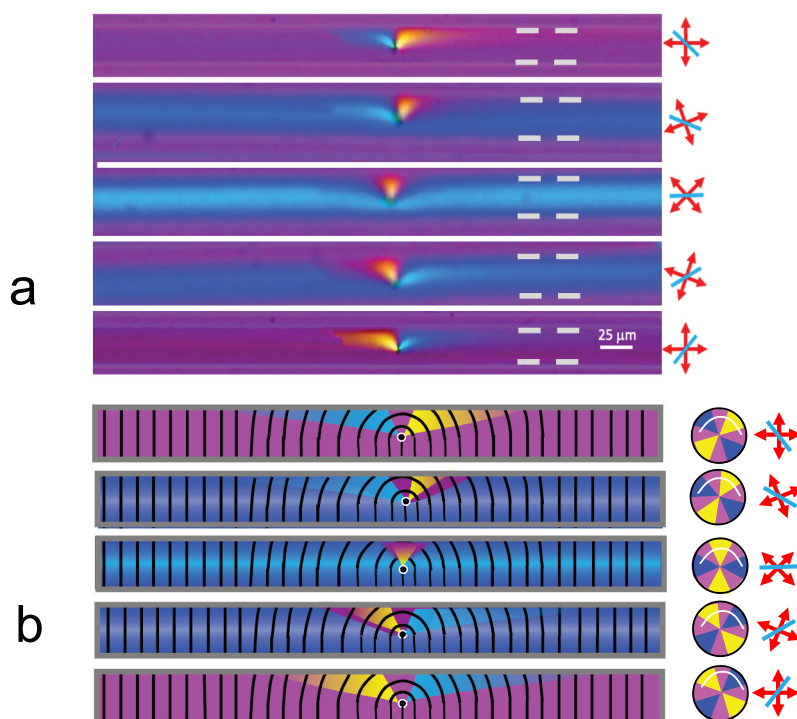


Figure 7. (Colour online) (a) Single defect from image 6a. Effect of rotating the polarisers and wave-plate. The double-headed red arrows indicate the orientation of the crossed polarisers and the blue diagonal line indicates the alignment of the slow axis of the λ plate. (b) The corresponding director field, with the black lines indicating the alignment of the axes of columns of molecules. The circular figures on the right indicate how the column alignments relate to the observed colours (as shown in Figure 3). Because of the simple, concentric semi-circular features in the director field, in this particular structure, the pattern of colours observed at each orientation relates directly to the upper half of the corresponding orientation diagram.

faster cooling parallels what was observed for the thin open films (Compare Figure 6(a,b) with Figure 3(a,c)) and what is seen when materials crystallise from solution or from the isotropic phase, where faster cooling often results in more, smaller crystals; more nucleation sites. Note that, the images in Figure 6 were obtained with the stripes parallel to one of the polarisers so that the aligned regions and the regions without LC are both magenta in colour. Rotation of the sample by $+45^\circ$ causes the stripes containing well-aligned LC to become blue and by -45° yellow, confirming that, over most of the sample, the columns (the director) lie across the stripes [22].

Isolated defects often form close to the edge of the stripe but, when they form part way across the stripe they have the appearance of $s = \frac{1}{2}$ defects (two brushes) rather than $s = 1$ defects (four brushes). The significant difference between the developable domains seen in Figure 6 and those in Figure 3 is that, whereas the boundary between the developable domain and rest of the sample in Figure 3 is sharp, those in Figure 6 are very diffuse. This is seen more clearly in Figure 7 in which one defect from Figure 6 is shown at higher magnification. It is shown as it appears using a range of orientations of the polarisers and wave-plate. Whereas in Figure 3 the director fields of the homeotropic ‘matrix’ and that of the developable domain are orthogonal to each other and there must be a sharp boundary between the two, in the stripes this is no longer the case. Here there must be a transition between a director field that circles the defect and one which is dictated by the surface curvature and that lies across the stripes. Because this involves splay (which is energetically expensive) the transition has to be gradual rather than abrupt. In the particular case shown in Figure 7, the ‘effect’ of the defect is still

apparent at a distance of at least $200\ \mu\text{m}$; particularly in the top and bottom lines of Figure 7(a) the ‘yellow’ and ‘blue’ regions extend over at least this distance from the centre of the defect.

Because the boundaries of the defects are so diffuse, because their effect extends over such a large distance, it becomes more favourable for two defects that are within a few hundred μm of each other to form on opposite sides of the stripe rather than on the same side of the stripe. This arrangement allows the director fields of the two domains to merge in a smooth manner.

When they are closer together than this, interaction between the two domains is more direct and there is probably little or no realignment of the director field towards the cross-stripe state. When they are close enough, the domains can match up directly in a manner first described by Bouligand [13], Figure 8.

Here, any given column follows a circular track centred on one defect until it reaches the solid red line (to which it is perpendicular) after which it either follows a circular track, centred on a different defect, which is curved in the opposite direction, Figure 8(a), a track curved in the same direction but with a different radius of curvature, Figure 8(b), or a straight line path, Figure 8(c). The only thing that changes on crossing the wall defined by the solid red line is the degree and/or direction of curvature of the columns. Although, within the de-wetted stripes, all of these possible situations are observed, the most frequently seen are those where the curvature alternates between right and left, Figure 8(a); where the defects alternate between one side of the stripe and the other. The resultant textures can also be visualised as a joined-up series of ‘opposed’ fans. Visually this creates a variety of zig-zag and wavy line optical textures and typical images (for HAT9 cooled at

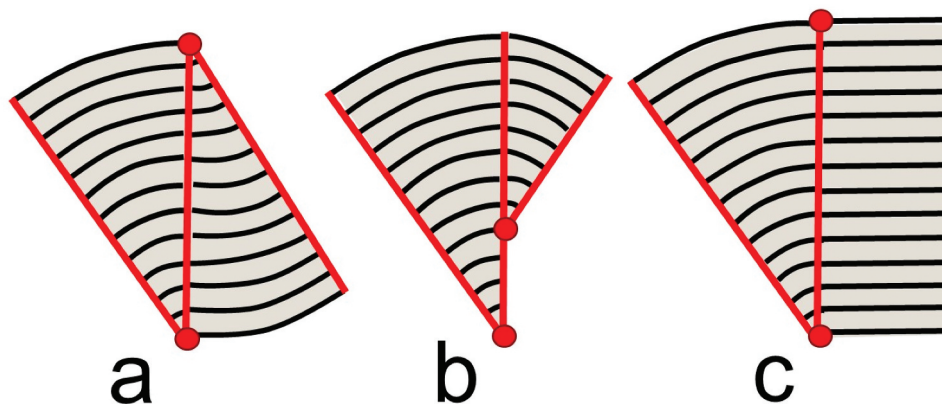


Figure 8. (Colour online) (a and b redrawn from Bouligand [13]) Schematic showing how segments of developable domains can be matched with each other in such a way that, at the dividing walls shown by the solid red lines, the columns are continuous and only the direction or degree of curvature changes.

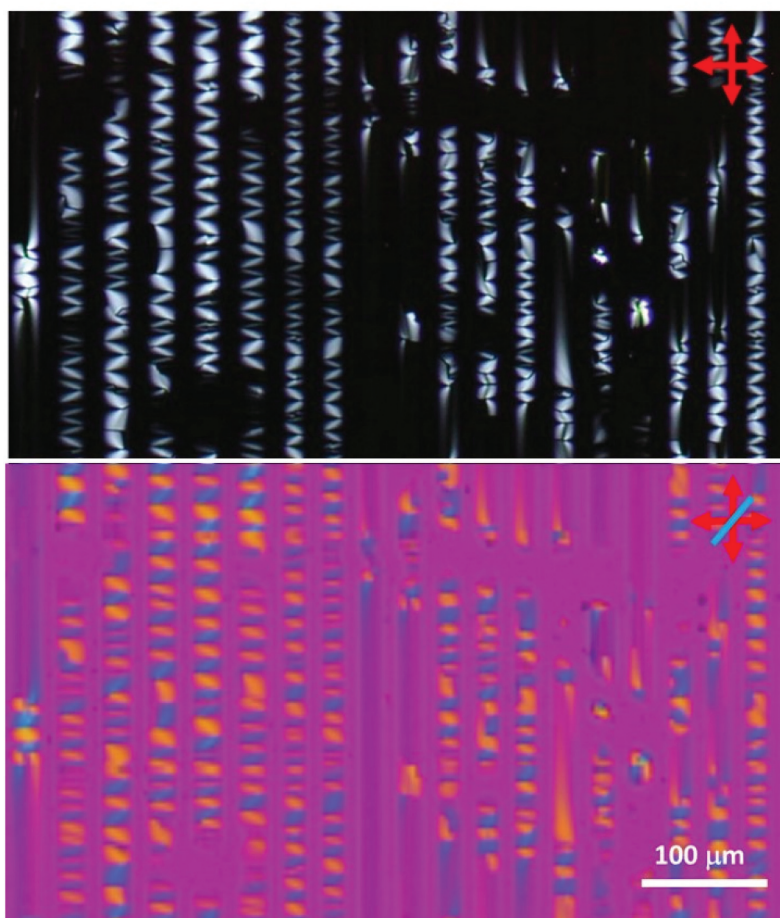


Figure 9. (Colour online) De-wetted sample of HAT9 on a patterned glass substrate which gives 25 μm (left hand side of the image) and 20 μm (right hand side) wide droplets with 10 μm wide spaces between them. Col_h phase at 70°C. Cooling rate from the isotropic phase 1°C/min. Transmission mode images, crossed polarisers with and without an added wave-plate. The blue line indicates the orientation of the slow axis of the wave-plate.

1°C/min) are shown in **Figure 9**. Characteristic of this structure is the observation of lines connecting the defects, which zig-zag along the stripe.

(Lower) Analysis of the optical textures above showing how the optical texture depends on the orientation of the crossed polarisers and wave-plate. Column (a) shows the orientation of the crossed polarisers. (b) The characteristic Maltese cross shown by a tangentially aligned circular array of birefringent material viewed between crossed polarisers. (c) The alternating head-to-tail pattern of developable domains in the specimen. (d) The appearance of the sample viewed between crossed polarisers – with the extinction positions shaded in grey. (e) The appearance of the specimen viewed between crossed polarisers with the red 1λ plate inserted. (f) The orientation diagrams for a circular array of birefringent material viewed between crossed polarisers with a red 1λ plate inserted. The white arcs indicate the range of orientations of the director,

which appear in each orientation (g) The 0 and 90° extinction positions for the crossed polarisers (shown in red), and the alignment of the slow axis of the red 1λ plate, indicated as a blue line.

As shown in the upper part of **Figure 10**, the appearance of these textures changes markedly as the orientation of the polarisers and wave-plate is varied relative to that of the sample; sometimes showing bands across the stripe rather than a zigzag. However, as shown in the lower half of the Figure, these changes are wholly as expected. One feature of these textures is that, when the defects are closely spaced, the lines connecting them appear to be rather narrow and uniform. However, if the defects are further apart, these features broaden and become leaf-like. The way in which these leaf-like features arise is shown in **Figure 11**

Some of the optical textures observed in these samples are strongly reminiscent of braid or of the kinds of decorative friezes associated with classical Greek and Roman architecture and since these are collectively

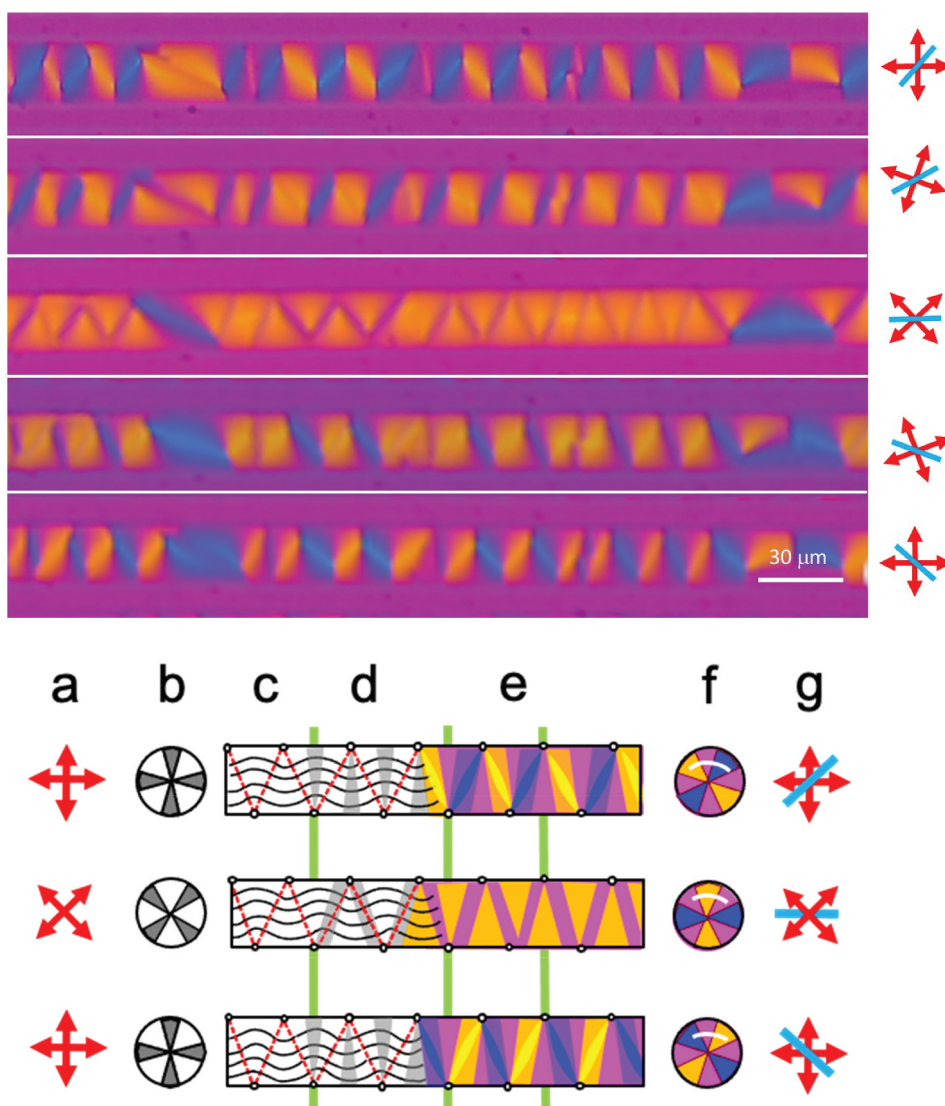


Figure 10. (Colour online) (Upper) Magnification of a single stripe from Figure 9 showing the effect of rotating the polarisers and wave-plate. The blue line indicates the orientation of the slow axis of the wave-plate.

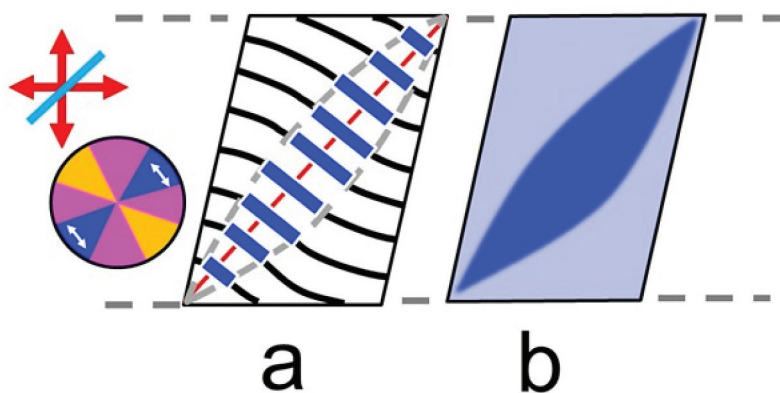


Figure 11. (Colour online) Origin of the leaf-shaped features seen in Figures 9 and 10. The broken red line indicates wall between two developable domains. The thick blue lines indicate the region where the director lies within a $\sim 5^\circ$ range of the 45° orientation to the crossed polarisers; the region where the polarisation colour is at its most intense.

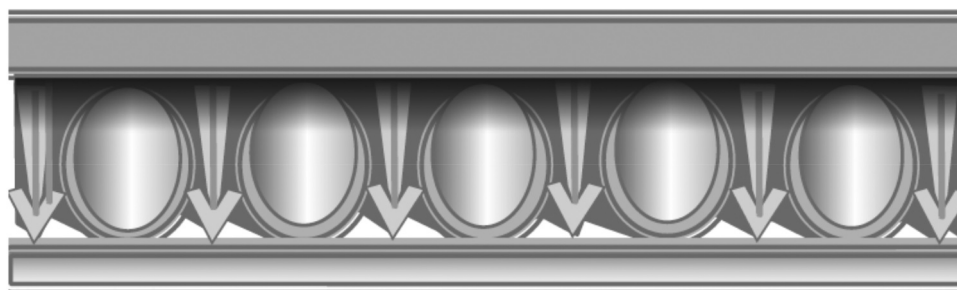


Figure 12. ‘Egg and dart’ pattern of the earliest type showing alternating shield and spear elements. Over the years the term ‘egg and dart’ came to be much more widely applied to different repeating patterns within a frieze.

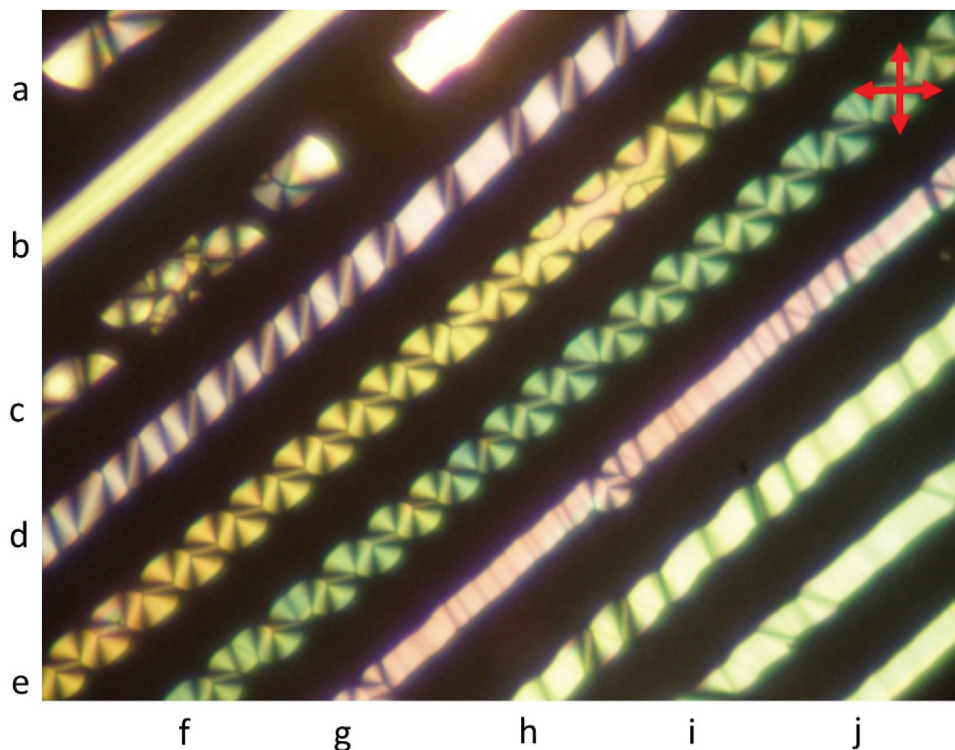


Figure 13. (Colour online) De-wetted sample of 1:1 PTP9:3 on a patterned silicon substrate giving 25 μm wide stripes of LC with 25 μm wide spaces between each stripe. Col_h phase at ca. 150°C. Reflection mode image, crossed polarisers.

known as ‘egg and dart’ patterns that, we suggest, is the most appropriate term to apply these textures. In their original basic form, Greek egg and dart decorations consisted of an alternating repeat of a circle, or oval shape and a stylised arrowhead, [Figure 12](#). Their origins date back at least two and a half thousand years and are debateable. One plausible suggestion is that the pattern originally represented the shields and spears of a phalanx of Greek infantry. The earliest known examples of egg and dart patterns date from Greek buildings of the 7th century BC in Greece, where it was incorporated in the capitals of the otherwise ultra-plain Ionic pillars. Over the following centuries, increasingly complex and intricate styles appeared. Egg and dart patterns reappeared on major public buildings during successive

waves of neo classical revivals throughout the Italian Renaissance, Georgian and Victorian times and, over the centuries, egg and dart has become a generic term for more-or-less any linear decoration with an alternating pattern of motif [39,40].

When there are alternating defects, most commonly, these are located at the edge of the stripe but in other cases they form lines close to the middle of the stripe as shown in [Figure 13](#) which is a reflection mode image for a sample of the CPI compound 1:1 PTP9:3 on a silicon substrate. Because of the colour of the substrate, the colours observed do not relate in a simple way to the Michel Levy series. However, the pastel tints suggest that they correspond to second or higher orders on the Michel-Levy chart and the uniform nature of the colour

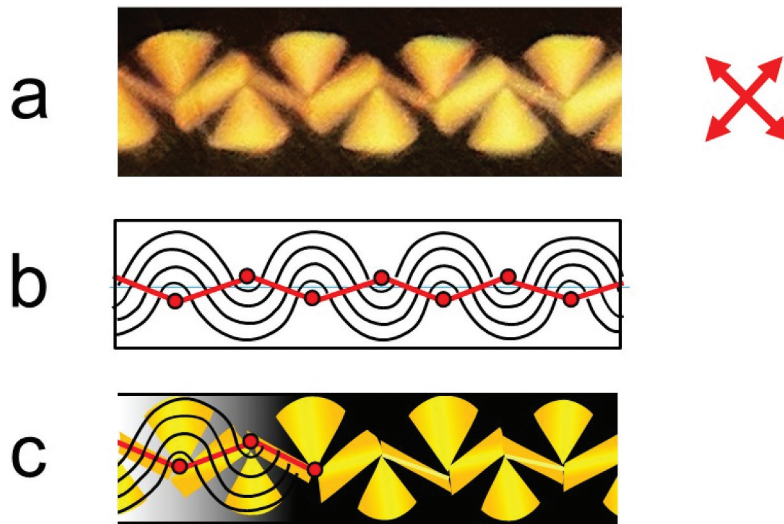


Figure 14. (Colour online) An enlarged region of stripe (e) in the micrograph shown in Figure 13. (b) The postulated sequence of segments of developable domains. The red lines indicate the domain boundaries, and the red dots indicate the Poles of the domains. (c) A sketch showing the appearance of the optical texture corresponding to (b).

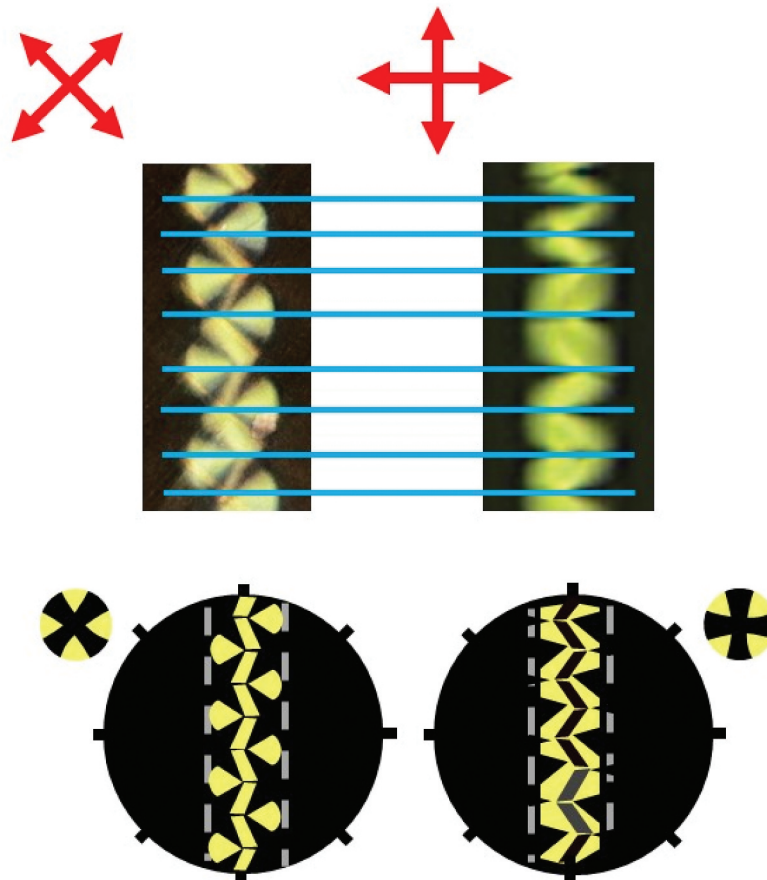


Figure 15. (Colour online) The effect of rotation of the sample (polarisers) on the texture seen in stripes f and e of Figure 13. Areas in which the material is not birefringent (and in which there is no separation into an ordinary and an extraordinary ray and hence no interference to create polarisation colours). These areas are black for all alignments: they do not change on rotation. In areas where the local director is parallel or perpendicular to the analyser the dark and light areas are interchanged every 45° of rotation.

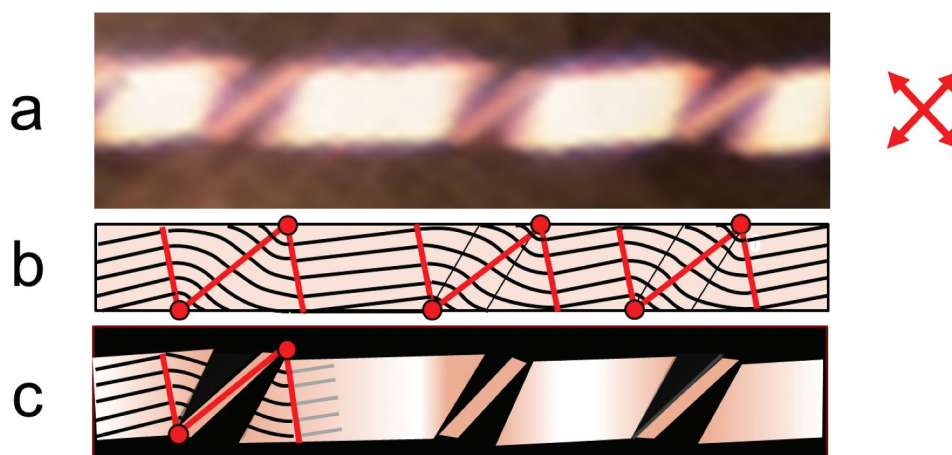


Figure 16. (Colour online) (a) An enlarged region of stripe (f) in the micrograph shown in Figure 13. (b) The postulated sequence of segments of developable domains. The red lines indicate the domain boundaries, and the red dots indicate the Poles of the domains. The pairs of fine black lines drawn diagonally crossing the two parallelograms on the right are the loci of points where the local director field lies at 45 degrees to the axis of the stripe (i.e. the extinction positions). (c) A sketch showing the appearance of the optical texture corresponding to (b).

across each stripe suggest rather flattened (low contact angle) droplets. Even when cooled slowly it was found that, for this sample, only a few of the stripes were uniformly aligned (stripes b and j), some are very disordered (stripes a and c), some show zig-zag patterns very similar to those in Figures 9 and 10 (stripes g and i), some have the appearance of twisted rope (stripes d and h), whilst others give alternating patterns in which the defects lie roughly in a line close to the middle of the stripe (stripes e and f)

In stripes e and f, although the defects still alternate, they form a line where they are much closer to the middle of the stripe. The probable director field is shown in Figure 14. The appearance of these stripes is very different when the sample or polarisers are rotated by 45 degrees, Figure 15. This arises because some of the dark areas are not birefringent whereas some correspond to areas where the local director is parallel or perpendicular to the analyser; some are unaffected by rotation but, for some, the dark and light areas are interchanged every 45°. Note that the way in which the curved semicircular features at the edges of the pattern in the left hand Figure are lost in the right hand Figure (the local director field lies parallel to an extinction direction).

Another interesting feature seen for the PTP9:3 system but not the HAT9 and HAT11 samples is the 'twisted rope' pattern seen in stripes d and h of Figure 13. Although there is the usual side-to-side alternation of the defects and, as usual, the spaces between the defects are irregular there appears to be an alternation between wide and narrow spaces. Also (in the

orientation shown) each defect is only associated with a single brush. This is incompatible with a director fields similar to that shown in Figure 10. The most probable director field is one composed of alternating circular and straight line segments as shown in Figure 16.

In these de-wetted stripes the most commonly observed features involve junctions between segments of domains of the type shown in Figure 8(a) in which, on crossing the dividing wall the direction of curvature of the columns changes from right to left (or *vice versa*); see for example Figures 10 and 14. However, in the case shown in Figure 16, on crossing the dividing wall, there is a change from curved to linear propagation of the columns of the type shown in Figure 8(c). Changes of the type shown in Figure 8(b), in which the direction of curvature remains the same but the focus changes are not often observed in these stripes. However, an example of this is shown in Figure 17 which is based on stripe g of Figure 13. Here, there is a small 'excursion' at the side of the stripe. The way in which the observed texture probably arises is shown in the schematics 17(b) and 17(c). This 'overspill' region was presumably triggered by some irregularity in the substrate surface and, on the assumption that buckling of the columnar structure is significant in the formation of egg and dart structures, it is interesting to note that this arrangement accommodates the longest possible length of continuous columns. Note the presence of two regions of parallel domain matching of the kind shown in Figure 8(b) in the distorted region in the centre of the Figure and, also, the slight asymmetry of the pattern.

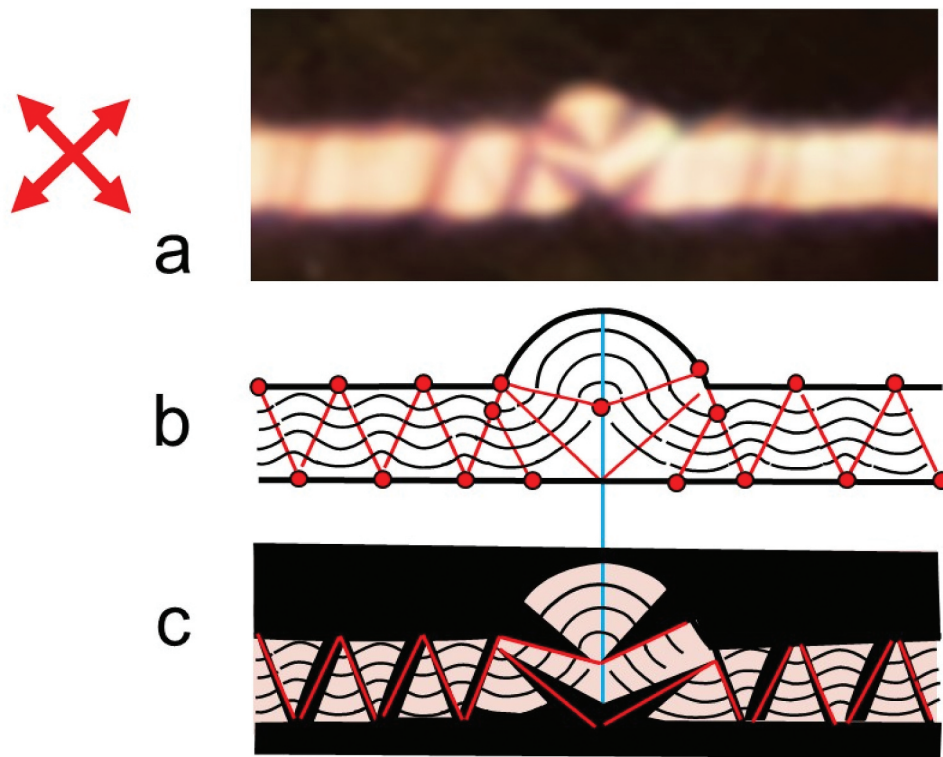


Figure 17. (Colour online) (a) An enlargement of the semicircular ‘overspill’ region from stripe g in Figure 13. (b) The postulated director field, with the domain boundaries shown as red lines and Poles as red dots. (c) A stylised representation of the corresponding optical texture, as viewed between crossed polarisers at a 45° orientation.

4. Conclusions

On a substrate patterned with alternating wetting and de-wetting stripes, the isotropic phase of a discotic LC de-wets to give an array of long narrow droplets. If the sample is then slowly cooled into its columnar phase, it is found that the columns align either across or (more rarely) along the stripes and this is one of the best ways to produce samples with a uniform ‘in-plane’ alignment of the director. However, defect-free alignment requires very narrow stripes ($\sim 10 \mu\text{m}$ or less) and very slow cooling ($< 1^\circ\text{C}/\text{min}$). This paper is concerned with the other extreme; it is concerned with faster cooling and wider stripes. Under these conditions many defects can be formed. It is found that these defects tend to alternate from side of the stripe to the other, giving rise to an array of different egg and dart optical textures. Although these appear to be very variable and quite complex, most of the apparent diversity and complexity arises because their appearance changes markedly depending on their orientation relative to the wave-plate and polarisers, Figures 10 and 15. To a first approximation, they can all be thought of as built up from just two basic sub-units; one in which the columns are straight and one in which they circle (or gently spiral) around a defect; the two units that are also the basic building blocks of

developable domains, Figure 1. These units can be matched up in a variety of different ways as shown in Figures 8, 10, 14, 16 and 17. At the junctions between these building blocks (indicated by the red lines in the Figures) the only change is a transition between linear and circular (or circular and circular) propagation of the columns. Within stripes junctions of the type shown in Figure 8(a,c) lead to textures in which the defects alternate between one side of the stripe and the other.

Whereas, this provides a simple explanation of how the egg and dart textures observed relate to the underlying director fields and ultimately to the ways in which developable domains can fit together it does not explain why they are formed or how they emerge from the isotropic medium. Neither does it explain how or whether these features relate to other zig-zag textures seen for columnar hexagonal phases such as the middle phases of lyotropic LCs, the columnar phases of tobacco mosaic virus [41] or the M phases of chromonic LCs [42]. It may simply be that (within the confines of the droplet) this is the thermodynamically favoured way for these domains to be matched up with each other. Arguments of this kind have been used to explain another example of alternating defects; the alternation of radial and hyperbolic defects in escaped radial director

fields of nematic LCs [21,43]. An alternative approach to the problem is to treat these features as paramorphotic; to argue that they are produced because the development of strain at the isotropic to columnar transition results in buckling of the columns. An argument of this type was first used by Rogers and Winsor to explain the zig-zag and herringbone textures seen for lyotropic middle phases and for tobacco mosaic virus [41] and was subsequently applied to M phases of chromonic LCs [42]. There are two similar explanations as to how such strain and buckling could arise; either as a result of preferential elongation of the columns as they grow from the isotropic or as a result of the unusual thermal expansion behaviour shown by at least some columnar phases [44] (positive coefficient of expansion along the columns but negative transverse to the columns). Both of these mechanisms provide a ready explanation as to why the features are particularly associated with more rapid cooling rates. They are also consistent with the form of the 'excursion' shown in Figure 17. However, the weakness of this explanation, as pointed out by Rogers and Winsor themselves, is that it is not easy to understand why these textures appear 'ready formed contemporaneously with the appearance of the columnar phase'; why, in most cases, there is no apparent change in the period of alternation as the sample cools.

Acknowledgments

We would like to thank Dr Peng Bao for making some of the patterned glass substrates.

RJB and SDE would like to acknowledge the financial support of the EPSRC with grant no: EP/EP/P023266/1.

Data Availability Statement

The dataset associated with this paper is available from the University of Leeds Data Repository and is located at <https://doi.org/10.5518/1037>.

Disclosure statement

No potential conflict of interest was reported by the author(s).

Funding

This work was supported by the Engineering and Physical Sciences Research Council [EP/EP/P023266/1].

References

- [1] Bushby RJ, Kawata K. Liquid crystals that affected the world: discotic liquid crystals. *Liq Cryst.* 2011;38(11–12):1415–1426.
- [2] Yan J, Rey AD. Texture formation in carbonaceous mesophase fibers. *Phys Rev E.* 2002 Feb 21;65(3):031713.
- [3] Yan J, Rey AD. Modeling elastic and viscous effects on the texture of ribbon-shaped carbonaceous mesophase fibers. *Carbon.* 2003 Jan 01;41(1):105–121.
- [4] Collyer AA. Lyotropic liquid-crystal polymers for engineering applications. *Mater Sci Technol.* 1990 Oct;6(10):981–992.
- [5] Carlton RJ, Hunter JT, Miller DS, et al. Chemical and biological sensing using liquid crystals. *Liq Cryst Rev.* 2013 Jun 01;1(1):29–51.
- [6] Sargazi M, Linford MR, Kaykhahi M. Liquid crystals in analytical chemistry: a review. *Crit Rev Anal Chem.* 2019 May 04;49(3):243–255.
- [7] Cronin T. Biosensors and liquid crystals. *Handb Liq Cryst.* 2014 Feb 26;8:1–21.
- [8] Frank FC. On the theory of liquid crystals [Article]. *Discuss Faraday Soc.* 1958;25(25):19–28.
- [9] Katsonis N, Marchenko A, Fichou D. Substrate-induced pairing in 2,3,6,7,10,11-Hexakisundecalkoxy-triphenylene self-assembled monolayers on Au(111). *J Am Chem Soc.* 2003 Nov 01;125(45):13682–13683.
- [10] De Cupere V, Tant J, Viville P, et al. Effect of interfaces on the alignment of a discotic liquid–crystalline phthalocyanine. *Langmuir.* 2006 Aug 01;22(18):7798–7806.
- [11] Al-Lawati ZH, Bushby RJ, Evans SD. Alignment of a columnar hexagonal discotic liquid crystal on self-assembled monolayers [Article]. *J Phys Chem C.* 2013 Apr;117(15):7533–7539.
- [12] Pisula W, Tomovic Z, El Hamaoui B, et al. Control of the homeotropic order of discotic hexa-peri-hexabenzocoronenes [Article]. *Adv Funct Mater.* 2005 Jun;15(6):893–904.
- [13] Bouligand Y. Defects and textures of hexagonal discotics. *J Phys.* 1980;41(11):1307–1315.
- [14] Kleman M. Developable domains in hexagonal liquid-crystals. *J Phys.* 1980;41(7):737–745.
- [15] Oswald P, Pieranski P. *Smectic and columnar liquid crystals.* Boca Raton (FL): Taylor and Francis; 2006.
- [16] Zhang RB, Zeng XB, Kim B, et al. Columnar liquid crystals in cylindrical nanoconfinement [Article]. *ACS Nano.* 2015 Feb;9(2):1759–1766.
- [17] Boden N, Bushby RJ, Headdock G, et al. Syntheses of new 'large core' discogens based on the triphenylene, azatriphenylene and hexabenzotrinaphthylene nuclei. *Liq Cryst.* 2001 Jan;28(1):139–144.
- [18] Bushby RJ, Lu ZB. Isopropoxy as a masked hydroxy group in aryl oxidative coupling reactions. *Synthesis-Stuttgart.* 2001 Apr;5:763–767.
- [19] Bushby RJ, Boden N, Kilner CA, et al. Helical geometry and liquid crystalline properties of 2,3,6,7,10,11-hexaalkoxy-1-nitrotriphenylenes. *J Mater Chem.* 2003;13(3):470–474.

- [20] Boden N, Bushby RJ, Lu ZB. A rational synthesis of polyacrylates with discogenic side groups. *Liq Cryst.* 1998 Jul;25(1):47–58.
- [21] Bao P, Paterson DA, Peyman SA, et al. Textures of nematic liquid crystal cylindrical-section droplets confined by chemically patterned surfaces [Article]. *Crystals.* 2021 Jan;11(1):65.
- [22] Bramble JP, Tate DJ, Revill DJ, et al. Planar alignment of columnar discotic liquid crystals by isotropic phase dewetting on chemically patterned surfaces. *Adv Funct Mater.* 2010 Mar 24;20(6):914–920.
- [23] Arikainen EO, Boden N, Bushby RJ, et al. Complimentary polytopic interactions [Article]. *Angew Chem-Int Ed.* 2000;39(13):2333–2336.
- [24] Lozman OR, Bushby RJ, Vinter JG. Complementary polytopic interactions (CPI) as revealed by molecular modelling using the XED force field [Article]. *J Chem Soc Perkin.* 2001 Sep 2;9:1446–1452.
- [25] Grelet E, Bock H. Control of the orientation of thin open supported columnar liquid crystal films by the kinetics of growth. *Europhys Lett.* 2006 Mar;73(5):712–718.
- [26] Gray GW, Goodby JWG. *Smectic liquid crystals; textures and structures.* Glasgow and London: Leonard hill; 1984.
- [27] Demus D, Richter L. *Textures of liquid crystals.* New York: Weinheim; 1978.
- [28] Knight DP, Vollrath F. Comparison of the spinning of selachian egg case ply sheets and orb web spider dragline filaments. *Biomacromolecules.* 2001 Jun 01;2(2):323–334.
- [29] Lydon JE. Silk: the original liquid crystalline polymer. *Liq Cryst Today.* 2004 Dec 01;13(3):1–13.
- [30] Pisula W, Kastler M, Wasserfallen D, et al. From macro- to nanoscopic templating with nanographenes. *J Am Chem Soc.* 2006 Nov 15;128(45):14424–14425.
- [31] Steinhart M, Zimmermann S, Goring P, et al. Liquid crystalline nanowires in porous alumina: geometric confinement versus influence of pore walls (vol 5, pg 432, 2005). *Nano Lett.* 2005 5; May(5): 995.
- [32] Safinya CR, Clark NA, Liang KS, et al. Synchrotron X-ray-scattering study of freely suspended discotic strands. *Mol Cryst Liq Cryst.* 1985;123(1–4):205–216.
- [33] Heiney PA, Fontes E, Dejeu WH, et al. Frustration and helicity in the ordered phases of a discotic compound. *Journal De Physique.* 1989 Feb 15;50(4):461–483.
- [34] Chiang LY, Safinya CR, Clark NA, et al. Highly oriented fibres of discotic liquid crystals. *J Chem Soc Chem Commun.* 1985;1985(11):695–696.
- [35] Safinya CR, Liang KS, Varady WA, et al. Synchrotron X-ray study of the orientational ordering D2-D1 structural phase-transition of freely suspended discotic strands in triphenylene hexa-normal-dodecanote. *Phys Rev Lett.* 1984;53(12):1172–1175.
- [36] Fontes E, Heiney PA, Ohba M, et al. Molecular disorder in columnar-phase discotic liquid crystal strands. *Phys Rev A.* 1988 Feb 15;37(4):1329–1334.
- [37] Fontes E, Heiney PA, Dejeu WH. Liquid-crystalline and helical order in a discotic mesophase. *Phys Rev Lett.* 1988 Sep 5;61(10):1202–1205.
- [38] Berreman DW. Solid surface shape and alignment of an adjacent nematic liquid-crystal [Article]. *Phys Rev Lett.* 1972;28(26):1683.
- [39] Meyer FS. *A handbook of ornament.* JM Classic ed. Huddersfield: Jeremy Mills Publishing; 2007.
- [40] Meyer FS. *Handbook of ornament. A grammar of art, industrial and architectural design in all its branches for practical as well as theoretical use.* New York: Dover Publications; 1957.
- [41] Rogers J, Winsor PA. Nature of striated textures encountered with middle (M1) and inverse middle (M2) liquid crystalline phases. Relationships between M1 phase of amphiphiles and ordered solution phase of tobacco mosaic virus [Article]. *J Colloid Interface Sci.* 1969;30(4):500.
- [42] Lydon JE. *Handbook of liquid crystals, chapter XVIII, chromonics.* First ed. Vol. 2B. Demus D, Goodby J, Gray GW et al., editors. Weinheim: Wiley-VCH; 1998.
- [43] Vilfan I, Vilfan M, Zumer S. Defect structures of nematic liquid-crystals in cylindrical cavities. *Phys Rev A.* 1991 Jun;43(12):6875–6880.
- [44] Kim HS, Choi SM, Pate BD, et al. Negative and positive anisotropic thermal expansions in a hexagonally packed columnar discotic liquid crystal thin film [Article]. *Chem Mater.* 2015 May;27(9):3417–3421.